INES'98

1998 IEEE International Conference on Intelligent Engineering Systems

September 17-19, 1998
Vienna, Austria

Proceedings

IHRT
Institute for Handling Devices and Robotics
Vienna University of Technology

ON THE OPTIMAL CONFIGURATION OF REDUNDANT MANIPULATORS

Fernando B.M. Duarte

Escola Superior de Tecnologia Viseu
Dep. Matemática, Campus Politécnico
3510 Viseu, Portugal
Tel: +351-32-4200500, Fax:+351-32-424651
Email:fduarte@mat.estv.ipv.pt

J.A.Tenreiro Machado

Faculdade de Engenharia da Universidade do Porto
Dep. de Eng. Electrotécnica e de Computadores
Rua dos Bragas, 4099 Porto Codex, Portugal
Tel: +351-2-2009913, Fax:+351-2-319280
Email: jtm@ fe.up.pt

Abstract —Redundant manipulators have some advantages when compared with classical arms because they allow the trajectory optimization, both on the free space and on the presence of obstacles, and the resolution of singularities. For this type of manipulators, the proposed kinematic control algorithms adopt generalized inverse matrices. In this line of thought, the generalized inverse control scheme is tested through several experiments that reveal the difficulties that often arise, namely by showing that we may get non-optimal arm configurations and chaotic-like motions. Motivated by these problems this paper presents a new method that optimizes the manipulability through a least square polynomial approximation to determine the joints positions. The experiments confirm the superior performance of the proposed algorithm for redundant and hyper-redundant manipulators.

I. INTRODUCTION

A kinematically redundant manipulator is a robotic arm possessing more degrees of freedom (*dof*) than those required to establish an arbitrary position and orientation of the end effector [1, 2]. Redundant manipulators offer several potential advantages over non-redundant arms. In a workspace with obstacles, the extra degrees of freedom can be used to move around or between obstacles and thereby to manipulate in situations that otherwise would be inaccessible.

When a manipulator is redundant, it is anticipated that the inverse kinematics admits an infinite number of solutions. This implies that, for a given location of the manipulator's end effector, it is possible to induce a self-motion of the structure without changing the location of the gripper. Thus, the arm can be reconfigured to find better postures for an assigned set of task requirements. Of course, redundant manipulators have disadvantages too. Their structure is more complex requiring sophisticated control algorithms that may lead to a higher computational load.

Most of the techniques for solving the kinematics of redundant manipulators that have been suggested control the end effector indirectly, through the rates at which the joints are driven, using the pseudoinverse of the Jacobian [5]. Nevertheless, these algorithms lead to a kind of chaotic motion with unpredictable arm configurations. Therefore, an important area of research remains open and more efficient algorithms must be envisaged.

Having these ideas in mind, the paper is organized as follows. Section 2 introduces the theory of generalized matrices and section 3 develops the kinematics of redundant manipulators. Based on these concepts, section 4 presents several experiments with two kinematic control schemes for redundant and hyper-redundant robots. Some results reveal a chaotic-like behaviour that is further analyzed in section 5. Finally, section 6 draws the main conclusions.

II. GENERALIZED INVERSES

For $\mathbf{A} \in \Re^{m \times n}$ and $\mathbf{X} \in \Re^{n \times m}$ the following relations are called the *Penrose conditions:*

$$\mathbf{AXA} = \mathbf{A} \quad (1)$$

$$\mathbf{XAX} = \mathbf{X} \quad (2)$$

$$(\mathbf{AX})^{\mathrm{T}} = \mathbf{AX} \quad (3)$$

$$(\mathbf{XA})^{\mathrm{T}} = \mathbf{XA} \quad (4)$$

A *generalized inverse* of matrix $\mathbf{A} \in \Re^{m \times n}$ is a matrix $\mathbf{X}=\mathbf{A}^{-} \in \Re^{n \times m}$ satisfying condition (1). On the other hand, a *reflexive generalized inverse* of matrix $\mathbf{A} \in \Re^{m \times n}$ is a matrix $\mathbf{X}=\mathbf{A}_{r}^{-} \in \Re^{n \times m}$ satisfying both conditions (1) and (2). Finally, *a pseudoinverse* of a matrix $\mathbf{A} \in \Re^{m \times n}$ (so-called *Moore-Penrose inverse*) is a matrix $\mathbf{X}=\mathbf{A}^{\#} \in \Re^{n \times m}$ satisfying conditions (1) through (4) [6].

III. KINEMATICS OF REDUNDANT MANIPULATORS

We consider a manipulator with n degrees of freedom whose joint variables are denoted by $\mathbf{q} = [q_1, q_2, ..., q_n]^T$. We assume that a class of tasks we are interested in can be described by m variables , $\mathbf{x} = [x_1, x_2, ..., x_m]^T$ ($m < n$) and that the relation between $\mathbf{q}$ and $\mathbf{x}$ is given by:

$$\mathbf{x} = f(\mathbf{q}) \tag{5}$$

where f is a function representing the direct kinematics. Differentiating (5) with respect to time yields:

$$\dot{\mathbf{x}} = \mathbf{J}(\mathbf{q})\dot{\mathbf{q}} \tag{6}$$

where $\dot{\mathbf{x}} \in \Re^m$, $\dot{\mathbf{q}} \in \Re^n$ and $\mathbf{J}(\mathbf{q}) = \partial f(\mathbf{q})/\partial \mathbf{q} \in \Re^{m \times n}$. Hence, from (6) it is possible to calculate a path $\mathbf{q}(t)$ in terms of a prescribed trajectory $\mathbf{x}(t)$ in the operational space. We assume that the following condition is satisfied:

$$\max \text{ rank } \{\mathbf{J}(\mathbf{q})\} = m \tag{7}$$

Failing to satisfy this condition usually means that the selection of manipulation variables is redundant and the number of these variables m can be reduced. When condition (5) is satisfied, we say that the degree of redundancy of the manipulator is $n-m$. If, for some $\mathbf{q}$

$$\text{rank } \{\mathbf{J}(\mathbf{q})\} < m \tag{8}$$

then the manipulator is in a singular state. This state is not desirable because, in this region of the trajectory, the manipulating ability is very limited. To analyze this problem it was proposed [4] the index $\mu = \sqrt{\det(\mathbf{J}\mathbf{J}^T)}$ as a measure of the manipulability.

A Inverse Kinematics

Most of the approaches for solving redundancy that have been proposed [3, 8] are based on the inversion of equation (6). A solution in terms of the joint velocities, is sought as

$$\dot{\mathbf{q}} = \mathbf{K}(\mathbf{q})\dot{\mathbf{x}} \tag{9}$$

where $\mathbf{K}$ is a suitable ($m \times n$) control matrix based on the Jacobian matrix

$$\dot{\mathbf{q}} = \mathbf{J}^{\#}(\mathbf{q})\dot{\mathbf{x}} \tag{10}$$

where $\mathbf{J}^{\#}$ is one of the generalized inverses of the $\mathbf{J}$. If $\mathbf{J}^{\#}$ is the pseudoinverse, satisfying conditions (1) through (4), it can be easily shown that a more general solution to equation (6) is given by

$$\dot{\mathbf{q}} = \mathbf{J}^{+}(\mathbf{q})\dot{\mathbf{x}} + \left[\mathbf{I} - \mathbf{J}^{+}(\mathbf{q})\mathbf{J}(\mathbf{q})\right]\dot{\mathbf{q}}_0 \tag{11}$$

where $\mathbf{I}$ is the ($n \times n$) identity matrix and $\dot{\mathbf{q}}_0$ is a ($m \times 1$) arbitrary joint velocity vector. The solution (11) is composed of two terms. The first term is relative to minimum norm joint velocities. The second term, the *homogeneous solution*, attempts to satisfy the additional constraints specified by $\dot{\mathbf{q}}_0$. Moreover, the matrix $\mathbf{I} - \mathbf{J}^{+}(\mathbf{q})\mathbf{J}(\mathbf{q})$ allows the projection of $\dot{\mathbf{q}}_0$ in the null space of $\mathbf{J}$. A direct consequence is that it is possible to generate internal motions that reconfigure the manipulator structure without changing the gripper position and orientation [7, 9]. Another aspect revealed by the solution of (10) is that repetitive trajectories in the operational space do not lead to periodic trajectories in the joint space. This is an obstacle for the solution of many tasks because the resultant robot configurations have similarities with those of an unstable system.

In order to solve this lack of repetition we adopt a distinct approach, entitled Open-Loop Manipulability (OLM) optimization method [10]. For a given point (x,y) in the operational space the new algorithm consists on computing the point in the joint space that maximizes μ. Given the symmetry of the robot kinematics, μ just depends on the radial distance $r = \sqrt{x^2 + y^2}$ of the point from the origin of coordinates and, therefore, we get the set of $n-m$ joint positions $q_j(r)$, ..., $q_{j+n-m}(r)$ optimal in a μ perspective. From these values and using a standard least squares method we calculate $n-m$ polynomials that fit approximately the data. Once fixed these variables, the other m joint positions can be calculate through a standard inverse kinematic algorithm.

The numerical calculation of the maximum manipulability (μ_{max}) and the corresponding joint values increase with the number of *dof*, but they can be computed off-line without imposing any load to real-time control.

IV. TRAJECTORY CONTROL OF REDUNDANT AND HYPER-REDUNDANT MANIPULATORS

In this section the formulations developed previously are employed for several manipulators.

The direct kinematics and the Jacobian of a k-link manipulator is:

$$\begin{bmatrix} x \\ y \end{bmatrix} = \begin{bmatrix} l_1 C_1 + l_2 C_{12} + l_3 C_{123} + \cdots + l_k C_{12\cdots k} \\ l_1 S_1 + l_2 S_{12} + l_3 S_{123} + \cdots + l_k S_{12\cdots k} \end{bmatrix} \tag{12 a}$$

$$\mathbf{J} = \begin{bmatrix} -l_1 S_1 - l_2 S_{12} - \cdots - l_k S_{1\cdots k} & \cdots & -l_k S_{1\cdots k} \\ l_1 C_1 + l_2 C_{12} + \cdots + l_k C_{1\cdots k} & \cdots & l_k C_{1\cdots k} \end{bmatrix} \tag{12 b}$$

where l_i is the length of link i, $S_{i\cdots k} = Sin(q_i + \cdots + q_k)$ and $C_{i\cdots k} = Cos(q_i + \cdots + q_k)$.

During the experiments, for all manipulators, it is considered $l_1 + l_2 + \ldots + l_k = 3$ and $l_1 = l_2 = \ldots = l_k$

In the closed-loop pseudoinverse's (CLP) method the joint positions can be computed through the time integration of the velocities according with the block diagram of the inverse kinematics algorithm depicted in Figure 1.

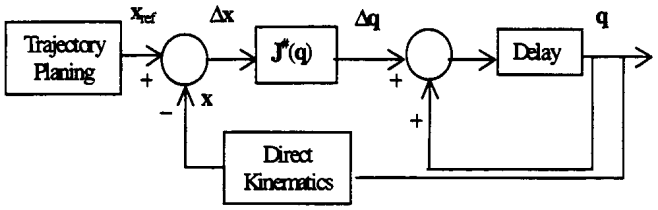

Fig. 1: Block diagram of the closed-loop inverse kinematics algorithm with the pseudoinverse (CLP).

In the next sub-sections we analyze for different manipulators the performances of the trajectory controllers based on the CLP and OLM methods. In this line of thought, we study the joint trajectories for the non-redundant $2R$, the redundant $3R$ and the hyper-redundant $4R$ and $5R$ robots, when subjected to a repetitive trajectory in the operational space according with the expression:

$$\mathbf{x}(t) = \begin{bmatrix} 0.5[1-\cos(\pi t)] \\ 0.5[2+\sin(\pi t)] \end{bmatrix}, 0 \le t \le 30 \qquad (13)$$

A. Non-Redundant Manipulator

Consider the $2R$ robot with an initial posture $\mathbf{q}(0) = [0.89\pi \quad -0.78\pi]^T$. The results of Figure 2 show the joint positions for the inverse kinematics algorithm based on (10) using the 'standard' 2×2 Jacobian matrix.

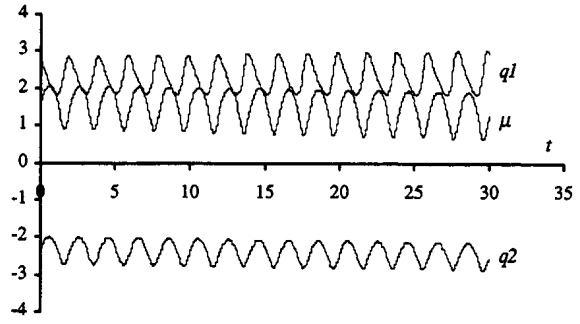

Fig. 2: The $2R$-robot joint positions *versus* time using the 'standard' Jacobian matrix.

As it is well known, in this case the joint trajectories and the manipulability index are repetitive along the *xy* circular motion.

B Redundant Manipulatosr

In this experiment we adopt the $3R$ arm with an initial posture $\mathbf{q}(0) = [\pi \quad -\pi/2 \quad -\pi/2]^T$. Figure 3 shows the joint positions for the inverse kinematic algorithm (10) using the CLP method.

In an alternative experiment, Figure 4 shows the joint positions for the inverse kinematic algorithm using the OLM method. In this case it is adopted the least square approximation polynomial $q_3 = 0.51r - 2.09$ for joint 3.

In these two experiments we have distinct results. When adopting the CLP, the manipulability is non-optimal and the joint trajectories exhibit sudden changes, which impose large joint velocity values. Moreover, the joint trajectories are non-repetitive leading to a kind of chaotic performance. When using the OLM procedure the trajectory is repetitive without large or fast transients.

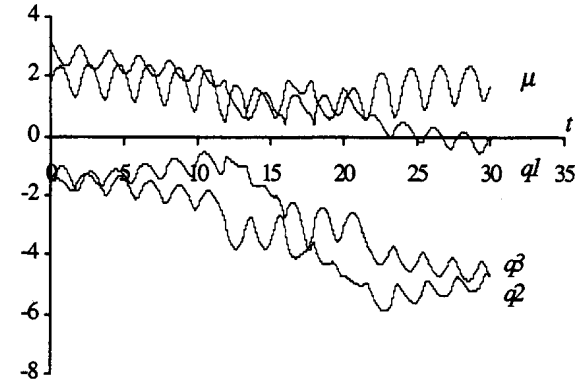

Fig. 3: The $3R$-robot joint positions *versus* time using the CLP method.

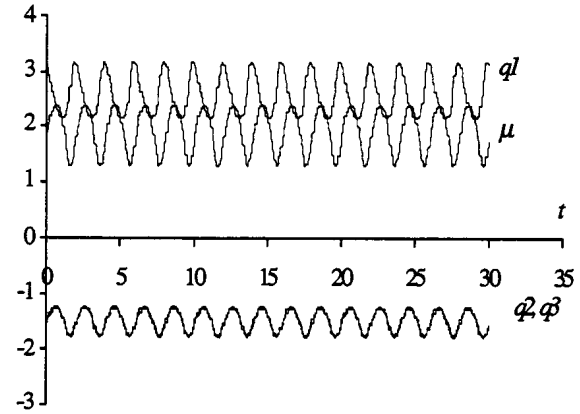

Fig. 4: The $3R$-robot joint positions *versus* time using the OLM method.

Comparing the Fourier transform of the joint velocities for both methods (Figs. 5 and 6) we conclude that the OLM scheme leads to an high first harmonic in the contrast with the chaotic-like signals of the CLP algorithm that reveal an heavier harmonic spectrum for the rest of the frequencies.

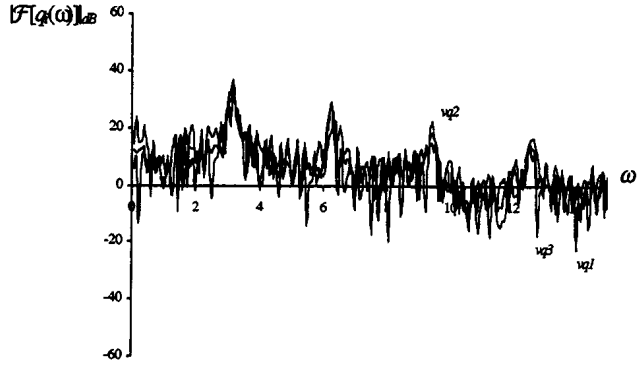

Fig. 5: Fourier spectrum of $\dot{q}(t)$ for the 3R-robot using CLP method.

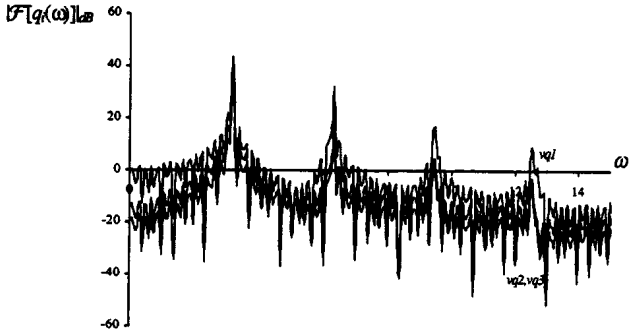

Fig. 6: Fourier spectrum of $\dot{q}(t)$ for the 3R-robot using OLM method.

C Hyper-Redundant Manipulators

In this sub-section we consider the 4R and 5R hyper-redundant manipulators under the control of the two previous methods. In the CLP method the manipulators configurations are:

4R-robot: $\mathbf{q}(0)=[0.97\pi \ -0.28\pi \ -0.41\pi \ -0.39\pi]^T$

5R-robot: $\mathbf{q}(0)=[-0.86\pi \ -0.34\pi \ -0.26\pi \ -\pi/3 \ -0.23\pi]^T$.

In the OLM algorithm we adopt least squares polynomial approximations.

For joints 3 and 4 of the 4R-robot we get:

- $q_3 = 0.41r^2 - 0.60r - 1.62$
- $q_4 = -0.24r^2 + 1.13r - 1.78$

For joints 3, 4 and 5 of the 5R-robot we get:

- $q_3 = 0.18r^3 - 0.64r^2 + 0.87r - 1.10$
- $q_4 = 0.14r^3 - 0.09r^2 - 0.04r - 1.41$
- $q_5 = 0.26r^3 - 1.22r^2 + 1.93r - 1.31$

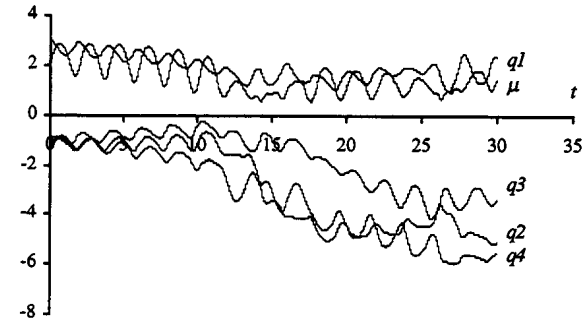

Fig. 7: The 4R-robot joint positions *versus* time using the CLP method.

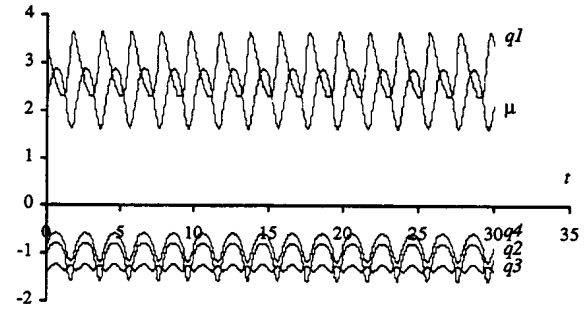

Fig. 8: The 4R-robot joint positions *versus* time using the OLM method.

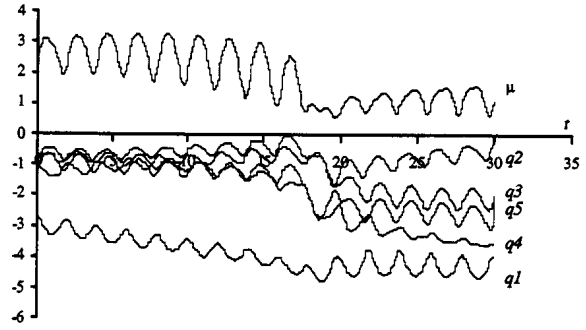

Fig. 9: The 5R-robot joint positions *versus* time using the CLP method.

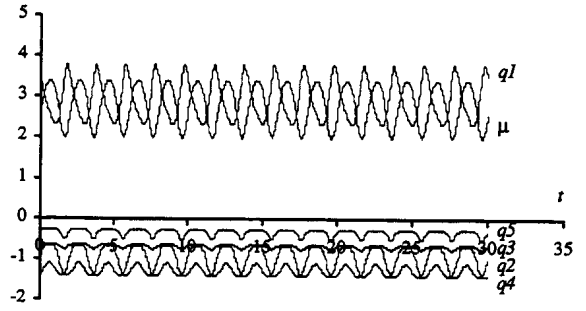

Fig. 10: The 5R-robot joint positions *versus* time using the OLM method.

In these experiments (Figs. 7 to 10) we observe performances similar to those revealed by the 3*R*-robot. Moreover, for the proposed method, the manipulability index seems to show better performances the higher the number of robot *dof*,

This conclusion is consistent with the fact that the larger the number of *dof* the higher the manipulability (for the appropriate robot configuration) as can be seen in Figure 11. Therefore, the OLM method taker advantage of this property while the CLP algorithm spans a large range of sub-optimal manipulability configurations (Fig 12).

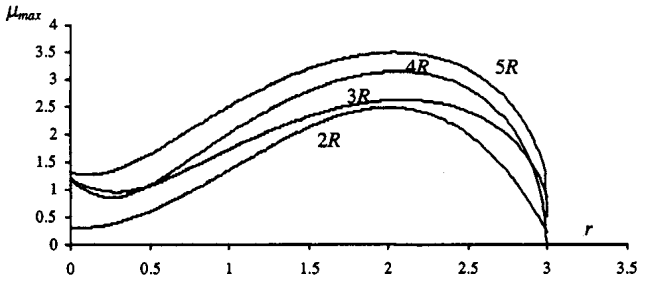

Fig. 11: Maximum manipulability index *versus* the radial distance for the 2*R*, 3*R*, 4*R* and 5*R* robots.

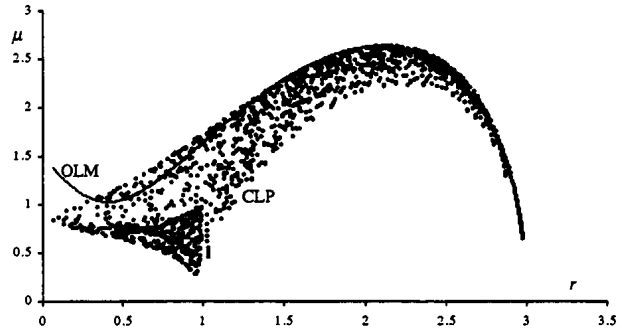

Fig. 12: Manipulability index *versus* the radial distance for the 3*R*-robot using the CLP and OLM methods.

V. ANALYZING THE CHAOTIC-LIKE RESPONSES OF THE CLP ALGORITHM

It was shown previously that the CLP algorithm leads to unpredictable arm configurations, with responses similar to those of a chaotic system.

For example, Figures 13-15 depict the phase-plane joint trajectories for the 3*R*-robot when repeating a circular motion, with center at $r = 1$, under the control of the CLP method. Besides the position and velocity drifts, leading to different trajectory loops, we have points that are "avoided". Such points correspond to arm configurations where several links are aligned and μ gets very low values. This characteristic is inherent to the pseudoinverse matrix because the 3*R*-robot was tested both under open-loop and closed-loop control, leading to the same type of behaviour. In order to gain further insight into the pseudoinverse chaotic nature, the robots under investigation were required to follow the cartesian repetitive circular motion for several radial distances (r). The phase-plane joint trajectories were then analyzed and their fractal dimension (*dim*) estimated through the standard box-counting method:

$$\dim S = \lim_{\varepsilon \to 0} \frac{\ln N(\varepsilon)}{\ln (1/\varepsilon)} \qquad (14)$$

where $N(\varepsilon)$ denotes the smallest number of bi-dimensional boxes of side length ε required in order to completely cover the plot surface S [11].

Figure 16 shows the resulting chart revealing that:

- for the CLP method we have *dim* near 2 due to the position and velocity drifts, in contrast with the OLM case where we have *dim* approximately 1.
- the fractal dimension diminishes in the higher radial distance (*i.e.* $r = 3$) where μ_{max} gets lower values.
- for each type of robot (2*R*, 3*R*, 4*R* and 5*R*) the fractal dimension is nearly the same, for all joints.

In conclusion, the CLP method leads to non-repetitive responses, with sub-optimal configurations. Therefore, in order to overcome those limitations other methods must be envisaged.

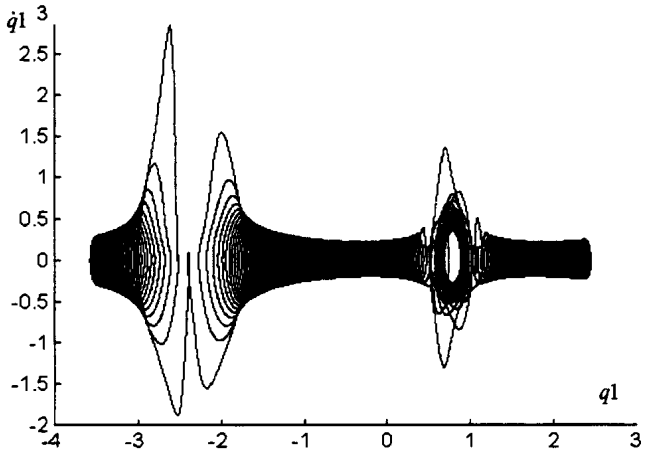

Fig. 13: Phase plane trajectory for the 3*R*- robot - joint 1, using the CLP method at $r = 1$, *dim* = 1.62.

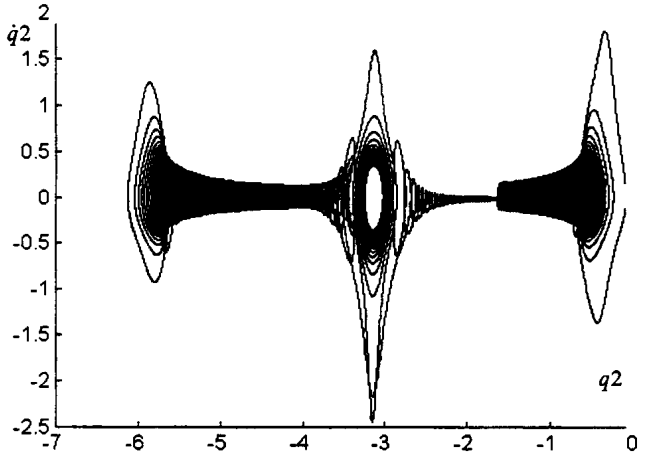

Fig. 14: Phase plane trajectory for the 3*R*- robot - joint 2, using the CLP method at $r = 1$, *dim* = 1.60.

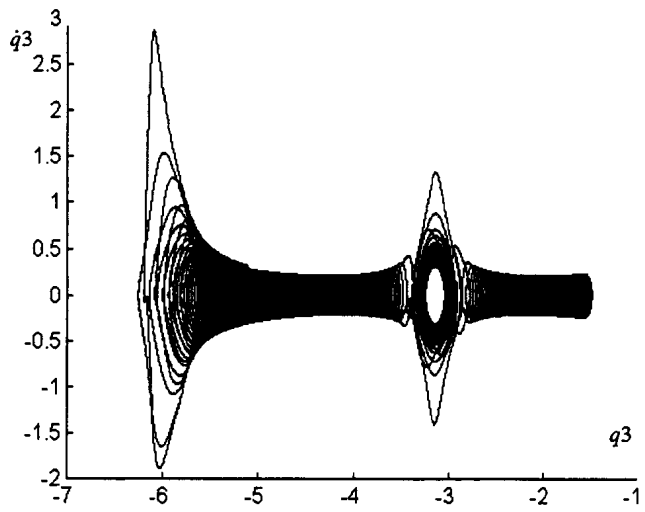

Fig. 15: Phase plane trajectory for the 3*R*- robot - joint 3, using the CLP method at $r = 1$, $dim = 1.63$.

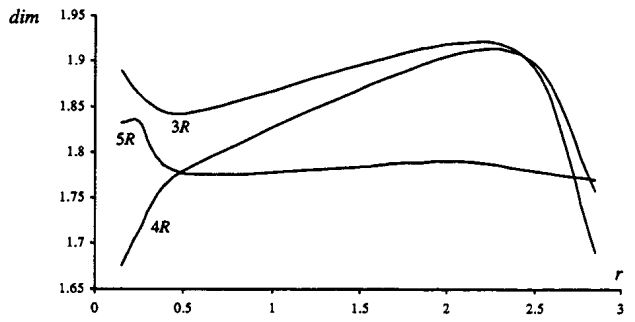

Fig. 16: Fractal dimension *versus* the radial distance for the 3*R*, 4*R* and 5*R* robots under CLP control.

VI. CONCLUSIONS

This paper discussed several aspects of the pseudoinverse-based control of redundant manipulators. An alternative based on the least squares polynomial approximation to the manipulability optimization was also developed. These techniques were applied in the trajectory control of redundant and hyper-redundant manipulators and their characteristics compared. The pseudoinverse scheme leads to non-optimal responses, both for the manipulability and the repeatability perspectives, while the new algorithm showed superior performances in both cases.

VII. REFERENCES

[1] E. Sahin Conkur, And Rob Buckingham "Clarifying the Definition of Redundancy as Used in Robotics", *Robotica*, vol. 15, pp. 583-586, 1997.

[2] Stefano Chiaverini "Singularity-Robust task-Priority Redundancy Resolution for Real Time Kinematic Control of Robot Manipulators", *IEEE Trans. Robotics Automation*, vol. 13, pp. 398-410, 1997.

[3] C.A Klein, and C. C Huang, "Review of Pseudoinverse Control for Use With Kinematically Redundant Manipulators", *IEEE Trans. Syst. Man, Cyber.*, vol. 13, pp. 245-250, 1983.

[4] Yoshikawa, T., "*Foundations of Robotics: Analysis and Control*", MIT Press, 1988.

[5] Y. Nakamura, "*Advanced Robotics: Redundancy and Optimization*", Addinson-Wesley, 1991.

[6] Keith L. Doty, C. Melchiorri and C. Bonivento, "A Theory of Generalized Inverses Applied to Robotics", *International Journal of Robotics Research*, vol. 12, pp. 1-19, 1993.

[7] Bruno Siciliano, " Kinematic Control of Redundant Robot Manipulators: A Tutorial", *Journal of Intelligent and Robotic Systems*, vol. 3, pp. 201-212, 1990.

[8] W.J.Chung, Y. Youm and W. K. Chung, "Inverse Kinematics of Planar Redundant Manipulators via Virtual Links With Configuration Index", *J. of Robotic Systems*, vol. 11, pp. 117-128, 1994.

[9] Sanjeev Seereeram and John T. Wen, "A Global Approach to Path Planning for Redundant Manipulators", *IEEE Trans. Robotics Automation*, vol. 11, pp.152-159, 1995.

[10] J.A.Tenreiro Machado and Fernando Duarte, "Trajectory Control of Redundant Manipulators", Proc. *COBEM 97*, Brazil, 1997.

[11] James Theiler, "*Estimating Fractal Dimension*", *Journal Optical Society of America*, vol. 7, n°6, pp. 1055-1073, 1990.

[12] J.A.Tenreiro Machado and Fernando Duarte, "Redundancy Optimization for Mechanical Manipulators", Proc. *AMC'98*, Coimbra, 1998.